A Refined Model of the Thyrotropin-Releasing Hormone (TRH) Receptor Binding Pocket. Experimental Analysis and Energy Minimization of the Complex between TRH and TRH Receptor†

Jeffrey H. Perlman,*,‡ Liisa J. Laakkonen,§ Frank Guarnieri,§ Roman Osman,§ and Marvin C. Gershengorn‡

Division of Molecular Medicine, Department of Medicine, Cornell University Medical College and The New York Hospital, New York, New York 10021, and Department of Physiology and Biophysics, Mount Sinai School of Medicine of the City University of New York, New York, New York 10029

Received September 14, 1995; Revised Manuscript Received April 8, 1996⊗

ABSTRACT: Seven transmembrane (TM) spanning, G protein-coupled receptors (GPCRs) appear to bind large glycoprotein hormones predominantly within their extracellular domains, small nonpeptidic ligands within the TM helical bundle, and peptide ligands within the extracellular domains and TM bundle. The tripeptide thyrotropin-releasing hormone (TRH, pyroGlu-His-ProNH$_2$) may bind entirely within the TM bundle of the TRH receptor (TRH-R). We have previously demonstrated direct binding contacts between the pyroGlu of TRH and two residues in TM helix 3 (TM-3) of TRH-R and proposed a model of the binding pocket of TRH-R [Perlman, J. H., Laakkonen, L., Osman, R., & Gershengorn, M. C. (1994) *J. Biol. Chem*. 269, 23383−23386]. Here, we provide evidence for two additional direct interactions between TRH and TRH-R. One interaction is between the aromatic ring of Tyr 282 of TM-6 and His of TRH. This is based on a large increase in the half-maximally effective concentration (EC_{50}) of TRH for stimulation of inositol phosphate formation by Y282A TRH-R and a loss of selectivity of this mutant receptor for TRH analogs substituted at His. We provide evidence for another interaction between Arg 306 of TM-7 and the terminal carboxamide of TRH. Using four direct interactions as anchors, a refined model of the TRH-R binding pocket was constructed using geometry optimization through energy minimization. A novel method for modeling GPCRs based on Monte Carlo and stochastic dynamics simulations is presented in the accompanying paper [Laakkonen, L. J., Guarnieri, F., Perlman, J. H., Gershengorn, M. C., & Osman, R. (1996) *Biochemistry 35,* 7651−7663].

Site-specific mutational studies of seven transmembrane (TM)[1] spanning, guanine nucleotide binding protein-coupled receptors (GPCRs) have been used to implicate amino acid residues within receptors as important for binding. The effect of a mutation may directly influence the binding pocket by substituting for a residue which directly binds the ligand. Alternatively, the mutation may indirectly affect the binding pocket by causing a conformational change which disrupts a binding interaction between a different residue and the ligand. It is critical to make this distinction in order to model the binding pocket accurately. One way to address this issue is through the use of complementary substitutions in the ligand and receptor. Loss of selectivity of a receptor, mutated at a specific residue, for a native ligand and an analog, which differs at a specific moiety from the native ligand, is consistent with the idea that the substituted receptor residue binds the substituted moiety of the native ligand. That is, a lack of full additivity of the effects of substitutions in the receptor and ligand suggests that the substituted receptor residue and substituted ligand moiety interact with each other. This approach has been used to demonstrate that an aspartate in TM-3 (Strader et al., 1991) and two serines in TM-5 of the β_2-adrenergic receptor (Strader et al., 1989a) directly bind the quaternary amine and catechol hydroxyl groups, respectively, of catecholamines. The binding pocket of GPCRs for peptides may be different than that of biogenic amines since peptides need not be positively charged and are larger. Direct interactions of peptides with GPCRs have been documented in a limited number of cases. For example, in the angiotensin II (AII) receptor, Lys 199 of TM-5 binds the terminal carboxylate of AII, Asp 281 of extracellular loop 3 (EC-3) binds Arg^2 of AII, and His 183 of EC-2 binds Asp^1 of AII (Noda et al., 1995; Feng et al., 1995); Glu 301 of EC-3 of the gonadotropin-releasing hormone receptor binds Arg^8 of gonadotropin-releasing hormone (Flanagan et al., 1994); Arg 397 of the large N-terminal extracellular domain of the luteinizing hormone receptor binds Lys 91 of the α-subunit of human choriogonadotropin (Ji et al., 1993); Arg 206 situated at the top of TM-5 of the C5A receptor binds the carboxy-terminal Arg of C5A hexapeptide analogs (DeMartino et al., 1995); and Tyr 115 of EC-1 of the vasopressin V1a receptor interacts with Arg^8 of arginine-

† This work was supported by National Institutes of Health Physician Scientist Award DK 02101 (to J.H.P.), Grant T32 DA 07135 (to F.G.), and Grant DK 43036 (to M.C.G. and R.O.).

* To whom correspondence should be addressed: Cornell University Medical College, 1300 York Ave., Room A328, New York, NY 10021. Telephone: 212 746-6272. Fax: 212 746-6289.

‡ Cornell University Medical College and The New York Hospital.

§ Mount Sinai School of Medicine of the City University of New York.

⊗ Abstract published in *Advance ACS Abstracts,* June 1, 1996.

[1] Abbreviations: TM, transmembrane; GPCR, G protein-coupled receptor; AII, angiotensin II; EC-3, extracellular loop 3, for example; TRH, thyrotropin-releasing hormone; TRH-R, thyrotropin-releasing hormone receptor; MeTRH, TRH in which *N*-τ-methylhistidine is substituted for His; Phe^{2}TRH, TRH in which Phe is substituted for His; Val^{2}TRH, TRH in which Val is substituted for His; Pyr^{3}TRH, TRH in which pyrrolidine is substituted for ProNH$_2$; IP, inositol phosphate; H-bond, hydrogen bond.

S0006-2960(95)02202-1 CCC: $12.00

vasopressin (Chini et al., 1995). However, in the majority of cases, substitutions have been made in the receptor alone, and importance for ligand binding has been assumed for residues without distinguishing between direct and indirect effects.

The thyrotropin-releasing hormone (TRH, pyroGluHis-ProNH$_2$) receptor (TRH-R) is a member of the GPCR superfamily. We have previously provided evidence for direct interactions between Tyr 106 and Asn 110 of TM-3 of TRH-R with pyroGlu of TRH (Perlman et al., 1994a,b). On the basis of this information and evidence that arginines of TM-6 and TM-7 were critical for binding (Perlman et al., 1995), a model was proposed for the TRH-R binding pocket (Perlman et al., 1994a). We have tested predictions of the initial model and provide evidence for two more direct interactions between TRH and TRH-R: Tyr 282 of TM-6 with His of TRH and Arg 306 of TM-7 with the terminal carboxamide of TRH. These four interactions have now been incorporated into a revised model of the TRH-R binding pocket. This represents, to our knowledge, the incorporation of the largest number of experimentally documented direct interactions between a peptide agonist and a GPCR into a model at an atomic level of detail. The model presented in this paper was constructed using geometry optimization through energy minimization. In the accompanying paper, a novel approach to modeling GPCRs using Monte Carlo and stochastic dynamics simulations is described (Laakkonen et al., 1996).

EXPERIMENTAL PROCEDURES

Materials. [^{3}H]MeTRH was obtained from DuPont. Myo[^{3}H]inositol was obtained from Amersham. TRH was from Calbiochem and MeTRH from Sigma. Val^{2}TRH and Phe^{2}TRH were obtained from Peninsula. Pyr^{3}TRH was the generous gift of Dr. T. K. Sawyer of Parke-Davis Pharmaceutical Research. Analogs were prepared *de novo* from precursors using solid-state synthesis and, therefore, contained no parent compounds as impurities. Restriction endonucleases were from New England Biolabs. The cloning vector pBluescript was from Stratagene and the expression vector pCDM8 from Invitrogen. Dulbecco's modified Eagle's medium and fetal calf serum were from Collaborative Research.

Mutagenesis. The full-length, mouse TRH-R cDNA in pBluescript (pBSmTRHR) (Straub et al., 1990) or pCDM8 (pCDM8mTRHR) (Gershengorn & Thaw, 1991) was used for mutation. Mutants were prepared by the polymerase chain reaction and were subcloned directly into pCDM8mTRHR (S113A and F199A TRH-Rs) or were subcloned into pBSmTRHR (Tyr 282 mutants) and then subcloned into pCDM8mTRHR after digesting with *Xho*I and *Not*I. Construction of Q105V, R283K, and R306K TRH-Rs was described previously (Perlman et al., 1994a, 1995). Mutant TRH-R sequences were confirmed by the dideoxy chain termination method.

Cell Culture and Transfection. COS-1 cells were maintained as described (Fujimoto et al., 1991) and were seeded 5 days prior to transfection at 30 000 cells/100 mm dish. Cells were transfected using the DEAE-dextran method as described (Straub et al., 1990) and maintained in Dulbecco's modified Eagle's medium with 10% fetal calf serum for 1 day, at which time cells were harvested and seeded into 12-well plates at 100 000 cells/well in Dulbecco's modified Eagle's medium with 5% fetal calf serum.

Receptor Binding Studies. One day after reseeding into 12-well plates, binding experiments were carried out in buffer with cells in the monolayer for 1 h at 37 °C as described (Perlman et al., 1992). The concentration of [^{3}H]MeTRH was 1 nM for cells expressing WT or S113A TRH-Rs and 5 nM for cells expressing Y282F TRH-Rs. B_{max} levels for WT, S113A, and Y282F TRH-Rs were similar. Inhibitory constants (K_i) were derived from competition binding experiments using the formula $K_i = (IC_{50})/(1 + ([L]/K_d))$, where IC_{50} is the concentration of unlabeled analog that half-displaces specifically bound [^{3}H]MeTRH and K_d is the equilibrium dissociation constant of TRH-R for [^{3}H]MeTRH. K_d s were obtained through competition binding of unlabeled MeTRH and, in the case of WT TRH-R, by saturation binding also. Curves were fitted by nonlinear regression analysis and drawn with the PRISM program (GraphPad Inc.).

Inositol Phosphate Formation. One day after transfection, cells in the monolayer in 12-well plates were labeled with 1 μCi of myo[^{3}H]inositol/mL. Stimulation of IP formation was measured 1 day later for 1 h at 37 °C by methods previously described (Perlman et al., 1994b). None of the analogs stimulated IP formation in untransfected cells. None of the mutant receptors showed constitutive activity. The zero point in the normalized figures refers to activity of receptor-expressing cells in the absence of agonist.

Construction of the Starting Structure of the Complex. We have constructed a model of the transmembrane (TM) domain of TRH-R (unpublished observations) on the basis of an analysis of GPCR sequences (Baldwin, 1993), the projection map of rhodopsin (Schertler et al., 1993), and Baldwin's prediction of the general structure of GPCRs (Baldwin, 1994). The model was constructed on a template of helical axes, which provided guidelines for positioning, tilting, and orienting the helices in a TM bundle. To test the template and the construction method, we built a model of rhodopsin, which agreed well with structural aspects derived from biochemical/mutational experiments (Khorana, 1992). In particular, the important interaction in rhodopsin between Lys-296 in TM-7 and Glu-113 in TM-3 was satisfied. We concluded, therefore, that our model of the TRH-R was sufficiently reliable to be used for a computational simulation to identify the binding pocket.

TRH was placed manually inside the helix bundle, and side chains of the ligand and the receptor were rotated manually to bring the interacting residues to close proximity. The pyroGlu in the ligand was placed to interact with Tyr 106 and Asn 110 in the receptor (Perlman et al., 1994a). The His of the ligand was neutral, consistent with the observed decrease in binding at lower pH values (Perlman et al., 1992). Tyr 282 in the receptor and the His of the ligand were positioned to maximize the overlap between the rings. Also, the guanidinium group of Arg 306 and the terminal carboxamide of the ligand were placed next to each other in a hydrogen-bonding (H-bonding) configuration.

Several initial structures were produced in the program MacroModel (Mohamadi et al., 1990), and the complexes were refined iteratively. First, distance constraints were applied to the individual H-bonds between the phenolic O−H (Tyr106) and O═C (pyroGlu) and between the guanidino

N−H (Arg 306) and the terminal O=C ($ProNH_2$). The flat-bottom constraint was defined as

$$E(\text{constraint}) = k(r - r_0)^2 \quad \text{for } (r_0 - \delta) \geq r \geq (r_0 + \delta)$$

and

$$E(\text{constraint}) = 0 \quad \text{for } (r_0 - \delta) < r < (r_0 + \delta)$$

where k is the force constant and δ is the tolerance within which the constraint is not applied. The force constant used in these simulations was 50 kJ/Å^2, r_0 was 2.0 Å, and δ was 0.5 Å. Stronger constraining force constants with smaller tolerance often contributed inappropriate deformation in the structure of the peptide; e.g., the peptide bonds in the ligand were converted to a *cis* form. The system was initially optimized by 1500 energy minimization steps with the flat-bottomed distant constraints and then followed by an additional 1500 steps without the constraints.

Next, the validity of the structures was evaluated by the presence or absence of contacts between the ligand and the selected residues in the receptor. The structures were accepted if Tyr 106 and Arg 306 formed H-bonds to the pyroGlu and $ProNH_2$, respectively, and Tyr 282 was sufficiently close to the His of the ligand. Structures with Asn 110 proximal to the pyroGlu, without necessarily forming an H-bond, were considered acceptable. The planarity of the peptide bonds was also checked, and deviations of more than 10° were not accepted. Total energy of the complex was found not to be consistent with structural acceptance criteria and therefore was not considered as a good indicator. On the other hand, the smoothness of the energy changes during minimization after the release of the constraints was found to be a reliable predictor. Drastic drops in energy upon release of the constraint correlated with loss of one of the contacts. Partially acceptable structures, i.e., those in which not all criteria were satisfied, were corrected manually to restore the lost interactions and served as input for the next cycle of minimizations. The process was continued until a complex that fulfilled all criteria simultaneously was achieved.

RESULTS

Our initial model of the TRH-R binding pocket was based on the observations that Tyr 106 strongly bound the ring carbonyl of pyroGlu, that Asn 110 weakly bound the ring N−H of pyroGlu, and that mutation of Arg 283 or Arg 306 affected binding. The model predicted a number of other interactions between TRH and TRH-R and between residues in TRH-R which could then be tested (Perlman et al., 1994a). The model proposed that Ser 113, Phe 199, and Arg 283 directly bound TRH, that Arg 306 formed intrareceptor interactions and indirectly maintained the conformation of the binding pocket, and that Tyr 282 formed a lid over the binding pocket. To begin to test these predictions, mutant TRH-Rs were constructed, expressed in COS-1 cells, and tested for binding and activation. Affinities were determined in intact cells through competition for binding of [^{3}H]-*N*-τ-methylhistidyl-TRH (MeTRH). MeTRH is an analog of TRH with 5−10-fold higher affinity and potency (Vale et al., 1973; Hinkle et al., 1974) which is used as radioligand. In these experiments, the K_d of WT TRH-R for MeTRH was 2.4 nM (Table 1, legend). The affinity of S113A TRH-R for MeTRH was 3.2 nM (95% confidence interval, 2.7−3.8 nM, $n = 4$), which is similar to that of WT TRH-R and indicates that Ser 113 is not important for binding. Mutation of Phe 199 and Tyr 282 markedly affected binding as evidenced by minimal specific binding of 5 nM [^{3}H]MeTRH by F199A or Y282A TRH-Rs. The K_d of Y282F TRH-R for MeTRH was 5-fold higher than WT TRH-R (Table 1, legend), indicating that the aromatic ring of Tyr 282 accounts for most of the observed decrease in binding associated with Y282A TRH-R. Previous results had indicated no specific binding of 5 nM [^{3}H]MeTRH by R283K or R306A TRH-Rs (Perlman et al., 1995).

Table 1: Binding of TRH Analogs by Wild-Type and Mutant TRH Receptors[a]

	TRH	Phe^{2}TRH	Val^{2}TRH	Pyr^{3}TRH
WT	0.028 (0.023−0.035) ($n = 3$)	1.3[b] (0.58−3.2) ($n = 2$)	14 (8.6−21) ($n = 3$)	18 (14−22) ($n = 3$)
Y282F	0.260 (0.200−0.340) ($n = 2$)	100 (72−140) ($n = 2$)	620 (400−970) ($n = 2$)	74 (61−90) ($n = 2$)

[a] The equilibrium constants of binding (K_is, μM) were determined through competitition binding with [^{3}H]MeTRH and are given as mean values with 95% confidence intervals and number of individual experiments in parentheses. Duplicate determinations of binding at each concentration of unlabeled ligand were obtained. The K_ds of [^{3}H]MeTRH binding to WT and Y282F TRH-Rs were 2.4 nM (1.8−3.0 nM, $n = 8$) and 11 nM (4.8−18 nM, $n = 7$), respectively. There was no specific binding of 5 nM [^{3}H]MeTRH by Q105V (see footnote *c*), F199A, Y282A, R283K (see footnote *c*), or R306A TRH-Rs (see footnote *c*). [b] From Perlman et al. (1994a). [c] In agreement with previously reported data (Perlman et al., 1994a, 1995).

To assess the affinities of mutant TRH-Rs which did not bind MeTRH with high affinity, the potencies of stimulation of inositol phosphate (IP) formation were measured. Relative potencies reflect relative affinities for ligand−receptor systems of equal efficacies (Limbird, 1986). For all mutant receptors described here, the maximal extent of IP formation was the same as WT TRH-R, which is consistent with their having similar efficacies. The EC_{50} of TRH for stimulation of IP formation by WT TRH-Rs was 0.54 nM. The EC_{50} of TRH for stimulation of S113A TRH-R was 0.73 nM (0.43−1.3 nM, $n = 3$), which is similar to that of WT TRH-R, and the EC_{50} of TRH for stimulation of Y282F TRH-R was 4.5 nM (Figure 2, Table 2), which is 8.3-fold higher than that of WT TRH-R. Thus, for those mutant TRH-Rs in which specific binding could be measured, the relative potencies reflected the relative affinities. Compared to WT TRH-R, the EC_{50}s of TRH for stimulation of F199A, R306A, R283K, and Y282A were 190-, 1900-, 5000-, and 94000-fold higher, respectively (Figure 2, Table 2). Thus, mutations of Phe 199, Arg 306, Arg 283, or Tyr 282 affect binding.

Substitution of a receptor residue may impact on the binding site directly or indirectly; i.e., the residue may directly contact TRH or may maintain the conformation of the binding pocket through intrareceptor interactions. To ascertain whether an effect is direct or indirect, the interactions of TRH analogs with TRH-Rs were studied (see above). To begin to study these interactions, competition between TRH analogs and [^{3}H]MeTRH for binding was measured in cells expressing WT TRH-Rs. TRH was substituted at His by Phe (Phe^{2}TRH) or Val (Val^{2}TRH) or at $ProNH_2$ by pyrrolidine (Pyr^{3}TRH). The only difference between Pyr^{3}TRH and TRH is replacement of the terminal carboxamide by hydrogen. Compared to TRH, the affinities of Phe^{2}TRH,

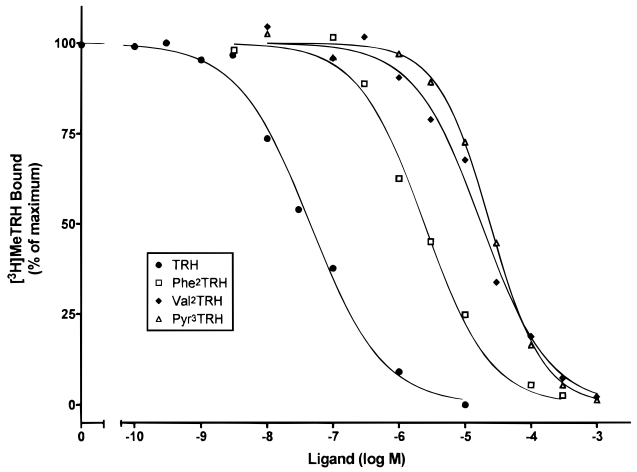

FIGURE 1: Binding of TRH analogs to wild-type TRH receptors. Competition binding of unlabeled TRH analogs for 1 nM [^{3}H]-MeTRH in cells expressing WT TRH-Rs. Data are expressed as percent of [^{3}H]MeTRH bound in the absence of unlabeled ligand. The K_d of [^{3}H]MeTRH for WT TRH-R is given in the legend to Table 1. Data for Phe^{2}TRH are from Perlman et al. (1994a).

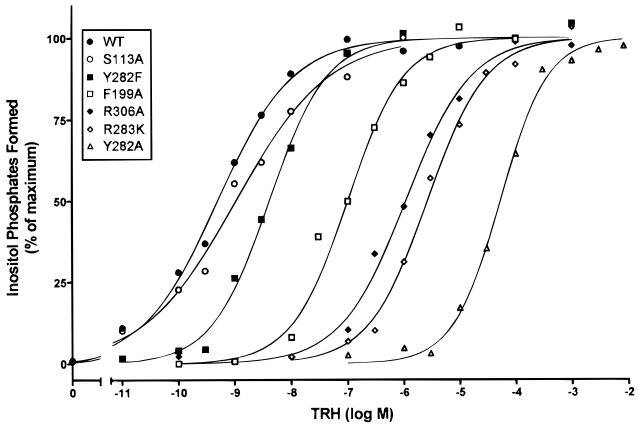

FIGURE 2: Activation of wild-type and mutant TRH receptors by TRH. Inositol phosphate formation in response to TRH. Data are expressed as percent of maximal inositol phosphate response. Fold stimulation of all TRH-Rs in response to TRH was similar (5.6 ± 0.4, mean ± standard error, $n = 51$).

Val^{2}TRH, and Pyr^{3}TRH were 46-, 500-, and 640-fold lower, respectively (Figure 1, Table 1). This confirms earlier radioligand binding and bioassay potency data indicating that His and the terminal carboxamide of TRH are critical for binding (Vale et al., 1973; Hinkle et al., 1974).

To test for an interaction between Phe 199 and His of TRH, the EC_{50}s of Phe^{2}TRH and Val^{2}TRH for stimulation of F199A TRH-Rs were measured and were observed to be 1800- and 8400-fold higher, respectively, than that of TRH (Table 2). Compared to WT TRH-R (see below), these shifts in EC_{50}s indicate no loss of selectivity for TRH analogs substituted at His and show that, although Phe 199 is important for binding, it does not appear to bind His of TRH directly.

The aromatic ring of Tyr 282 may be involved in binding as there was a much larger affinity decrease observed with an Ala, than a Phe, substitution. The importance of the aromatic ring was confirmed by Ser and Asn substitutions of Tyr 282. The EC_{50}s of Y282S and Y282N TRH-Rs were 31 μM (24−40 μM, $n = 5$) and 90 μM (66−120 μM, $n = 7$), respectively, which are 57 000- and 170 000-fold higher, respectively, than that of WT TRH-R. It was possible that an interaction between the aromatic ring of Tyr 282 and His of TRH was responsible for this effect. To test this hypothesis, the EC_{50}s of TRH, Phe^{2}TRH, and Val^{2}TRH were compared for WT and Y282A TRH-Rs. For WT TRH-R, the EC_{50}s of Phe^{2}TRH and Val^{2}TRH were 89- and 960-fold higher than that of TRH (Figure 3a, Table 2), indicating that relative potencies did reflect relative affinities for these analogs. For Y282A TRH-R, the EC_{50}s of Phe^{2}TRH and Val^{2}TRH were only 2.5- and 24-fold higher, respectively, than that of TRH (Figure 3b, Table 2). Thus, there was a marked loss of selectivity of Y282A TRH-R for either TRH analog substituted at His, consistent with the idea that Tyr 282 interacts with His of TRH.

To test whether the aromatic ring or the phenolic hydroxyl of Tyr 282 was interacting with His of TRH, the affinities of TRH analogs were compared for Y282F TRH-R. The K_is of Phe^{2}TRH and Val^{2}TRH were 380- and 2400-fold higher, respectively, than that of TRH (Table 1), and the EC_{50}s of Phe^{2}TRH and Val^{2}TRH were 4200- and 130 000-fold higher, respectively, than that of TRH (Table 2). Thus, there was no loss of selectivity of Y282F TRH-R for TRH analogs substituted at His. The data provide evidence for an interaction between the aromatic ring of Tyr 282 and His of TRH.

The initial model had predicted that Arg 283 bound the terminal carboxamide of TRH. To test this hypothesis, the EC_{50}s of TRH and Pyr^{3}TRH were compared for WT and R283K TRH-Rs. The R283K mutant TRH-R, rather than another Arg 283 mutant, was studied because we had shown previously that substitutions by residues which did not contain an N−H group resulted in inactive receptors (Perlman et al., 1995). For WT TRH-R, the EC_{50} of Pyr^{3}TRH was 1200-fold higher than that of TRH, indicating that relative potency reflected relative affinity for this analog (Figure 4a, Table 2). For R283K TRH-Rs, the EC_{50} of Pyr^{3}TRH was 740-fold higher than that of TRH (Table 2), indicating no loss of selectivity for this TRH analog which lacks the terminal carboxamide. Thus, Arg 283 does not bind the terminal carboxamide of TRH.

Our data indicated that mutation of Arg 306 affected binding and it was possible that an interaction with the terminal carboxamide of TRH was responsible for this effect. To test this hypothesis, the EC_{50}s of TRH and Pyr^{3}TRH were compared for R306A TRH-R. The EC_{50} of Pyr^{3}TRH was only 59-fold higher than that of TRH in cells expressing R306A TRH-Rs compared to 1200-fold in cells expressing WT TRH-Rs (Figure 4b, Table 2), indicating a loss of selectivity for this TRH analog. Thus, the data suggest that Arg 306 binds the terminal carboxamide of TRH.

The initial model had proposed that Gln 105 interacted with Arg 306 and that substitutions of Gln 105 could indirectly affect TRH binding. Evidence that substitutions of Gln 105 could indirectly affect the binding pocket included substantial decreases in affinity noted for replacements of Gln 105 by large residues and only a 3-fold loss of affinity observed for Q105A TRH-R (Perlman et al., 1994a). For example, there was no specific binding of [^{3}H]MeTRH by Q105V TRH-R (Table 1, legend). To test for an interaction of Gln 105 with Arg 306, the EC_{50}s of TRH and Pyr^{3}TRH were compared for Q105V TRH-R. For Q105V TRH-R, the EC_{50} of TRH was 1.7 μM and the EC_{50} of Pyr^{3}TRH was only 65-fold higher than that of TRH (Table 2), indicating a loss of selectivity of Q105V TRH-R for TRH and

Table 2: Activation of Wild-Type and Mutant TRH Receptors by TRH Analogs[a]

	TRH	Phe[2]TRH	Val[2]TRH	Pyr[3]TRH
WT	0.00054 (0.00045−0.00065) ($n = 17$)	0.048 (0.034−0.068) ($n = 4$)	0.52 (0.39−0.77) ($n = 7$)	0.64 (0.50−0.81) ($n = 4$)
Q105V	1.7[b] (1.4−2.0) ($n = 2$)	154 (114−209) ($n = 2$)	580 (450−750) ($n = 2$)	110 (82−140) ($n = 2$)
F199A	0.10 (0.080−0.14) ($n = 4$)	180 (120−280) ($n = 2$)	840 (720−970) ($n = 2$)	300 (240−370) ($n = 2$)
Y282A	51 (44−60) ($n = 8$)	130 (100−170) ($n = 2$)	1200 (1000−1300) ($n = 5$)	>3000 - ($n = 2$)
Y282F	0.0045 (0.0034−0.0061) ($n = 3$)	19 (10−36) ($n = 2$)	590 (390−880) ($n = 2$)	57 (34−97) ($n = 2$)
R283K	2.7 (2.0−3.5) ($n = 5$)	730 (490−1100) ($n = 3$)	1000 (870−1200) ($n = 2$)	2000 (1600−2500) ($n = 5$)
R306A	1.0 (0.74−1.4) ($n = 5$)	120 (91−160) ($n = 2$)	360 (300−430) ($n = 2$)	59 (44−78) ($n = 5$)

[a] The EC_{50} values of activation, expressed in μM, are given as mean values with 95% confidence intervals and number of individual experiments in parentheses. Duplicate or triplicate determinations at each concentration of ligand were obtained. [b] In agreement with EC_{50} of 1.5 μM previously reported (Perlman et al., 1994a).

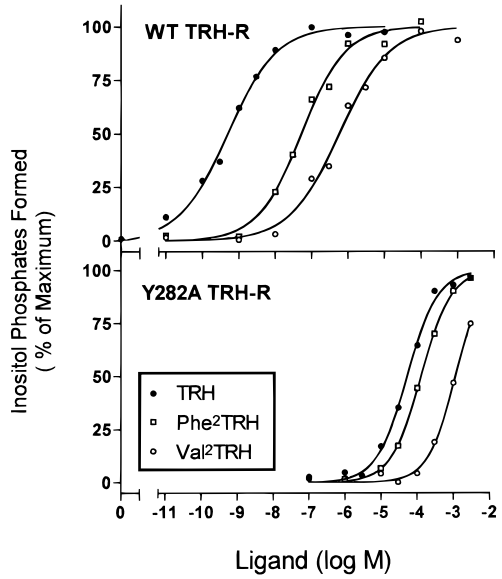

FIGURE 3: Activation of wild-type (a, upper panel) and Y282A (b, lower panel) TRH receptors by TRH and analogs substituted at His of TRH. Inositol phosphate formation in response to TRH, Phe[2]TRH, and Val[2]TRH. Data are expressed as percent of maximal inositol phosphate response to TRH.

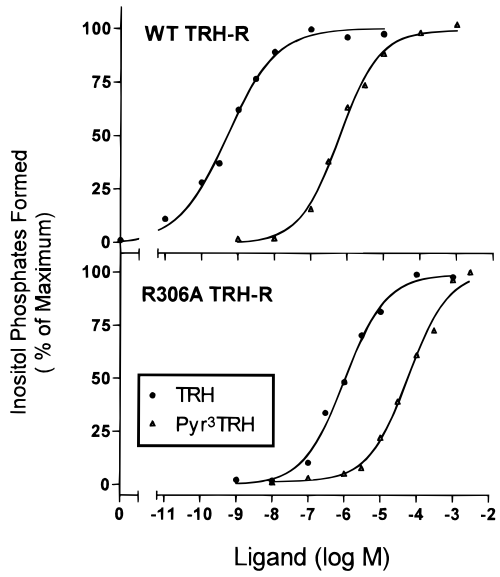

FIGURE 4: Activation of wild-type (a, upper panel) and R306A (b, lower panel) TRH receptors by TRH and analogs substituted at $ProNH_2$ of TRH. Inositol phosphate formation in response to TRH and Pyr[3]TRH. Data are expressed as percent of maximal inositol phosphate response to TRH.

Pyr[3]TRH. Combined with a similar loss of selectivity of R306A TRH-R and the demonstrated indirect effect of Gln 105 substitutions, the data are consistent with an interaction between Val 105 and Arg 306 in the mutant Q105V TRH-R. This confirms the proximity of Gln 105 to Arg 306 (Figure 5).

Experiments were performed to support the contention that Tyr 282 and Arg 306 were specifically interacting with His and the terminal amide, respectively, of TRH. Evidence supporting the specificity of the interaction between His of TRH and Tyr 282 of TRH-R was obtained by measuring the EC_{50}s of activation (Table 2) of Phe[2]TRH and Val[2]TRH for TRH-Rs substituted at positions other than Tyr 282 and comparing to TRH for WT and mutant TRH-Rs. Compared to TRH, the shifts to the right with these analogs for Q105V, F199A, R283K, or R306A TRH-Rs were similar to or larger than that of WT TRH-R. This supports the proposal that the interaction between Tyr 282 and His of TRH is specific and direct. Similarly, evidence supporting the specificity of the interaction between the terminal carboxamide of TRH and Arg 306 of TRH-R was obtained through measuring the K_is of binding (Table 1) or EC_{50}s of activation (Table 2) of Pyr[3]TRH with TRH-Rs substituted at positions other than Arg 306 (or Q105V TRH-R, see above) and comparing to TRH for WT and mutant TRH-Rs. Compared to TRH, the shifts in K_is of binding or EC_{50}s of activation of F199A, Y282F, and R283K TRH-Rs were similar to or larger than that of WT TRH-R. In the case of Y282A TRH-R, a dose−response curve of Pyr[3]TRH with Y282A TRH-R was not possible due to the very low affinity interaction; however,

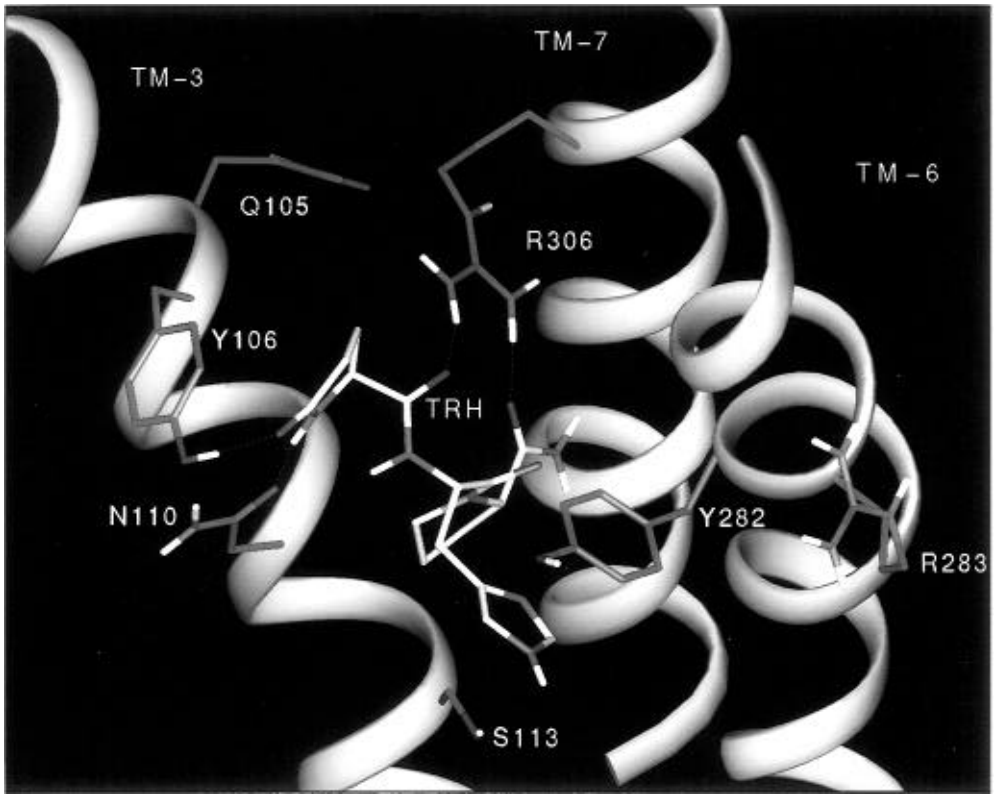

FIGURE 5: Model of the complex between TRH and TRH receptor. On the basis of experimentally determined interactions between TRH and TRH-R, an energy-minimized model of the transmembrane bundle was constructed as described in Experimental Procedures. For clarity, transmembrane helices (TMs) 1, 2, 4, and 5 were omitted from the view. Binding interactions are described in the text. Color code: light green, TMs; dark green, selected receptor residue side chain carbons; yellow, TRH carbons; red, oxygens; blue, nitrogens; white, hydrogens.

the EC_{50} was at least 3 mM. These data are consistent with the idea that the interaction between Arg 306 and the terminal carboxamide of TRH is specific and direct.

Thus, we have provided evidence for direct interactions between the aromatic ring of Tyr 282 and His of TRH (this paper), between Arg 306 and the terminal carboxamide of TRH (this paper), between the phenolic hydroxyl of Tyr 106 and the ring carbonyl of pyroGlu of TRH (Perlman et al., 1994b), and between Asn 110 and the ring N−H of pyroGlu (Perlman et al., 1994a). We have developed a model of the unoccupied TRH-R constructed from a rhodopsin template which was based on an analysis of GPCR sequence homologies (Baldwin, 1993). Using the four documented direct interactions as anchors, TRH was interactively docked in the core of the unoccupied receptor and the structure was geometry optimized through energy minimization. The final minimized structure is shown in Figure 5. The stability of the simulated ligand−receptor structure and retention of experimentally documented interactions support the idea that the positioning of the TM helices is correct. The model shows the following: (1) TRH binds within the TM helical bundle. (2) The hydroxyl group of Tyr 106 forms an H-bond to the ring carbonyl group of pyroGlu of TRH. (3) The side chain carbonyl of Asn 110 forms an H-bond to the ring N−H of pyroGlu of TRH. (4) Tyr 282 interacts with His of TRH. (5) The guanidino group of Arg 306 forms an H-bond to the terminal carboxamide of $ProNH_2$ of TRH. (6) Gln 105 of TM-3 is within close proximity of Arg 306 of TM-7. (7) The guanidino group of Arg 306 is predicted to form an H-bond to the peptidyl carbonyl group of pyroGlu of TRH. (8) Ser 113 and Arg 283 do not bind TRH. Of note, the energy minimization procedure does not take into account the dynamic properties of the ligand, receptor, or bound complex. To address this issue, mixed mode Monte Carlo and stochastic dynamics simulations were performed and the results described in the accompanying paper (Laakkonen et al., 1996).

DISCUSSION

We have used an approach of complementary substitutions in the receptor and ligand to provide evidence for direct interactions between TRH and TRH-R. In this manner, we have identified four interactions and used them to construct a model of the binding pocket of TRH-R. In general, the interpretation of the effects of changes in a receptor and its ligand is most straightforward for two ideal cases. In one ideal case, the affinity decreases resulting from substitutions in the receptor and ligand may or may not be similar, but importantly, there is no loss in the ability of the mutant receptor to distinguish between the native ligand and analog. This is consistent with the idea that there is no interaction between the substituted receptor residue and the substituted ligand moiety. This was found for substitution of Phe 199 in TRH-R and His in TRH and refuted the prediction of the initial model of the TRH/TRH-R complex (Perlman et al., 1994a) that showed an interaction between these two residues. In the other ideal case, there are similar affinity decreases resulting from substitutions in the receptor and ligand and a complete loss of ability of the mutant receptor to distinguish between the native ligand and analog. This would be consistent with the idea that an interaction between the substituted receptor residue and the substituted ligand moiety fully accounts for the affinity loss. The interactions involving Tyr 282, for example, fall into an intermediate

category. The effects of mutating Tyr 282 and substituting for His differ in magnitude, but Y282A TRH-R partially loses the ability to distinguish between TRH and analogs substituted at His. That is, the rightward shift of Val^2TRH or Phe^2TRH compared to TRH is far less for the Y282A mutant than for WT TRH-R. Thus, the data indicate that Tyr 282 does interact with His but that both Tyr 282 and His appear to interact with other groups as well.

The validity of this approach cannot be fully verified until crystal structures are available for the TRH/TRH-R complex. At present, the only high-resolution crystallographic image of a 7-TM protein is that of bacteriorhodopsin (Henderson et al., 1990) which, however, is not a GPCR and does not share sequence homology with GPCRs. The only image of a GPCR is a low-resolution, two-dimensional projection map of rhodopsin (Schertler et al., 1993; Schertler & Hargrave, 1995). In the absence of crystallographic data, molecular modeling provides the best means of integrating experimental observations and generating testable hypotheses regarding the structure of a GPCR, in particular, the potential interactions between ligand and receptor and between residues within a receptor. When crystallographic data are available, the functional relevance of the structural data will still need to be evaluated. For example, it has been demonstrated that 85% of the binding affinity of the growth hormone receptor can be accounted for by 33% of the residues observed to contact growth hormone by crystallographic studies (Cunningham & Wells, 1993; DeVos et al., 1992).

The projection map of rhodopsin is the most direct data to date regarding the topology of GPCRs (Schertler et al., 1993; Schertler & Hargrave, 1995). Indirect evidence for the proposed GPCR topology includes the demonstration of interactions between TMs 1 and 7 in the α_2 adrenergic and muscarinic receptors (Suryanarayana et al., 1992; Liu et al., 1995); reestablishment of ligand binding or activation through reciprocal mutations in TMs 2 and 7 of the gonadotropin-releasing hormone receptor [Zhou et al., 1994, but see Cook et al. (1993)], the serotonin $5HT_{2a}$ receptor (Sealfon et al., 1995), and TRH-R (unpublished experiments); and substitution of the function of the counterionic Glu in TM-3 of rhodopsin by an Asp in TM-2 (Rao et al., 1994). Our data demonstrating direct contact sites for ligand on three different helices of a GPCR confirm that TMs 3, 6, and 7 are in proximity to each other. Moreover, we show that Gln 105 of TM-3 and Arg 306 of TM-7 are in close proximity. These data support the general structure proposed for the GPCR superfamily (Baldwin, 1993, 1994).

It has been proposed that TMs 3, 5, 6, and 7 are important for binding of various small ligands (Baldwin, 1994). Tyrosine 506 of TM-6 of the muscarinic receptor M3 receptor, homologous to Tyr 282 of TRH-R, has been proposed to form part of a hydrophilic ring binding the acetylcholine ester group (Wess et al., 1992). However, direct interactions between agonists and residues in TMs 6 and 7 have been demonstrated in only a small number of receptors. Proposals regarding the importance of TMs 6 and 7 have been based on effects of receptor mutations without complementary agonist substitutions. These residues include Phe 290 of TM-6 of the β-adrenergic receptor (Strader et al., 1989b), which is homologous to Arg 283 of TRH-R. Similarly, although the importance of a residue homologous to Arg 306 in TM-7 has been shown, for example, with regard to selectivity of adrenergic antagonists (Suryanarayana & Kobilka, 1993), a specific direct interaction between this residue and ligand has not been demonstrated.

The location of the binding pocket for peptide ligands is less well defined than that of smaller nonpeptidic agonists. A major anchor in TRH-R for binding is one position removed from the counterion residue of GPCRs for biogenic amine neurotransmitters, and the other end of TRH is intercalated between TMs 6 and 7 rather than TMs 5 and 6 as proposed for biogenic amines and adenosine receptors (Schwartz, 1994). Of note, other documented direct contacts between TM residues and peptides include Lys 199 of TM-5 of the AII receptor with the terminal carboxylate of AII and Arg 206 of TM-5 of the C5A receptor with the terminal Arg of C5A hexapeptide analogs. Thus, our findings represent the first demonstrations in GPCRs of direct interactions between TMs 3, 6, and 7 and peptide agonists.

The geometry-optimized model predicts a number of interactions between TRH and TRH-R, for example, an interaction between Arg 306 and the peptidyl carbonyl group of pyroGlu, that will be tested in future experiments. This indicates an essential aspect of the interplay between the experimental and modeling methodologies. Predictions generated by the model are tested and the model refined accordingly. The model can thus be viewed as an evolving working hypothesis that provides a framework within which to interpret experimental findings.

Han and Tashjian have proposed that Asn 110 is not important for binding, based, in part, on the fact that mutation of Asn 110 to Asp resulted in no decrease in potency of TRH (Han & Tashjian, 1995). This finding, however, is consistent with our model in which the carbonyl of Asn 110 (which is retained in Asp) binds the ring N−H of pyroGlu. We were able to demonstrate this interaction, which is the weakest of the four direct interactions between TRH and TRH-R that we have identified, through a decreased ability of N110A TRH-R to distinguish between TRH and an analog in which the ring N−H of pyroGlu was replaced by O (Perlman et al., 1994a). Subsequently, we tested an analog in which the ring N−H was replaced by a methylene group, and similar results were obtained (unpublished experiments).

Han and Tashjian have also proposed that the ring N−H of the pyroGlu of TRH binds to Asn 289, which is at the juncture of TM-6 and the third extracellular loop (Han & Tashjian, 1995). In their experiments, mutation of Asn 289 to Ala resulted in only a 10-fold lower potency of TRH, suggesting that such an interaction involving Asn 289 would be weak. Moreover, they measured potency by assaying stimulation of chloride currents within 1 min of exposure to agonists in *Xenopus laevis* oocytes made to express WT and mutant TRH-Rs. Their data, therefore, more specifically address rapid effects of TRH and may not be quantitatively similar to measurements of binding at equilibrium. Nonetheless, it is possible that TRH could bind to TRH-R in more than one way and weak interactions may be different in different states of binding. This idea is consistent with data indicating that TRH binding to TRH-R changes from a lower to a higher affinity interaction with time (Hinkle & Kinsella, 1982).

All peptide agonists larger than three amino acids, characterized to date, have been shown to bind at least in part to extracellular domains of their receptors [for review, see Strader et al. (1995)]. Reported direct contacts of extracellular residues of GPCRs with peptide agonists include

EC loops of the angiotensin II, gonadotropin-releasing hormone, luteinizing hormone, and vasopressin receptors. However, it is possible that GPCR agonists must interact with TM domains to effect activation and that extracellular binding serves to position the agonist for binding to TM residues. In contrast, TRH, perhaps because of its small size, appears to have its major interactions within the TM domains. Since, in general, contact with TM residues of GPCRs may be needed to achieve activation, the interactions of TRH with TRH-R may serve as a prototype for activating interactions of peptide agonists with TM domains of GPCRs.

Since the atomic coordinates of bacteriorhodopsin are known (Henderson et al., 1990), it is usually used as a template in modeling GPCRs, but for the reasons cited above, a template based on rhodopsin may be preferable. Our models of the unoccupied and occupied receptor are based on a rhodopsin template, and the methodology we have developed for fitting specific helices onto the template is generalizable to any GPCR. We have described a model in which the structure has been geometry optimized through energy minimization. The minimization process does not allow for sampling of conformations separated by large energy barriers and may, therefore, select a local rather than a global minimum energy state. This problem has been addressed for the TRH-R through the use of Monte Carlo and stochastic dynamics simulations which are described in the accompanying paper (Laakkonen et al., 1996). To our knowledge, this is the first use of such simulations in the modeling of a GPCR.

The process of refining a model through testing of generated hypotheses engenders confidence in the model and provides predictions for further testing. The result is the most detailed information available regarding the structure of the receptor binding pocket in the absence of direct crystallographic data. On the basis of four demonstrated contacts between TRH and TRH-R, we have constructed an energy-minimized model of the TRH-R. A novel approach to modeling of GPCRs appears in the accompanying paper.

REFERENCES

Baldwin, J. M. (1993) *EMBO J. 12*, 1693.

Baldwin, J. M. (1994) *Curr. Opin. Cell Biol. 6*, 180.

Chini, B., Mouillac, B., Ala, Y., Balestre, M. N., Trumpp-Kallmeyer, S., Hoflack, J., Elands, J., Hibert, M., Manning, M., Jard, S., & Barberis, C. (1995) *EMBO J. 14*, 2176.

Cook, J. V., Faccenda, E., Anderson, L., Couper, G. G., Eidne, K. A., & Taylor, P. L. (1993) *J. Endocrinol. 139*, R1.

Cunningham, B. C., & Wells, J. A. (1993) *J. Mol. Biol. 234*, 554.

DeMartino, J. A., Konteatis, Z. D., Siciliano, S. J., Van Riper, G., Underwood, D. J., Fischer, P. A., & Springer, M. S. (1995) *J. Biol. Chem. 270*, 15966.

DeVos, A. M., Ultsch, M., & Kossiakoff, A. A. (1992) *Science 255*, 306.

Feng, Y.-H., Noda, K., Saad, Y., Liu, X., Husain, A., & Karnik, S. S. (1995) *J. Biol. Chem. 270*, 12846.

Flanagan, C. A., Becker, I. I., Davidson, J. S., Wakefield, I. K., Zhou, W., Sealfon, S. C., & Millar, R. P. (1994) *J. Biol. Chem. 269*, 22636.

Fujimoto, J., Straub, R. E., & Gershengorn, M. C. (1991) *Mol. Endocrinol. 5*, 1527.

Gershengorn, M. C., & Thaw, C. N. (1991) *Endocrinology 128*, 1204.

Han, B., & Tashjian, A. H., Jr. (1995) *Biochemistry 34*, 13412.

Henderson, R., Baldwin, J. M., Ceska, T. A., Zemlin, F., Beckmann, E., & Downing, K. H. (1990) *J. Mol. Biol. 213*, 899.

Hinkle, P. M., & Kinsella, P. A. (1982) *J. Biol. Chem. 257*, 5462.

Hinkle, P. M., Woroch, E. L., & Tashjian, A. H. (1974) *J. Biol. Chem. 249*, 3085.

Ji, I., Zeng, H., & Ji, T. H. (1993) *J. Biol. Chem. 268*, 22971.

Khorana, H. G. (1992) *J. Biol. Chem. 267*, 1.

Laakkonen, L. J., Guarnieri, F., Perlman, J. H., Gershengorn, M. C., & Osman, R. (1996) *Biochemistry 35*, 7651−7663.

Limbird, L. E. (1986) in *Cell surface receptors: A short course on theory and methods*, Martinus Nijhoff Publishing, Boston, Dordrecht, Lancaster.

Liu, J., Schoneberg, T., van Rhee, M., & Wess, J. (1995) *J. Biol. Chem. 270*, 19532.

Mohamadi, F., Richards, N. G. J., Guida, W. C., Liskamp, R., Lipton, M., Caufield, C., Chang, G., Hendrickson, T., & Still, W. C. (1990) *J. Comput. Chem. 11*, 440.

Noda, K., Saad, Y., Kinoshita, A., Boyle, T. P., Graham, R. M., Husain, A., & Karnik, S. S. (1995) *J. Biol. Chem. 270*, 2284.

Perlman, J. H., Nussenzveig, D. R., Osman, R., & Gershengorn, M. C. (1992) *J. Biol. Chem. 267*, 24413.

Perlman, J. H., Laakkonen, L., Osman, R., & Gershengorn, M. C. (1994a) *J. Biol. Chem. 269*, 23383.

Perlman, J. H., Thaw, C. N., Laakkonen, L., Bowers, C. Y., Osman, R., & Gershengorn, M. C. (1994b) *J. Biol. Chem. 269*, 1610.

Perlman, J. H., Laakkonen, L., Osman, R., & Gershengorn, M. C. (1995) *Mol. Pharmacol. 47*, 480.

Rao, V. R., Cohen, G. B., & Oprian, D. D. (1994) *Nature 367*, 639.

Schertler, G. F. X., & Hargrave, P. A. (1995) *Proc. Natl. Acad. Sci. U.S.A. 92*, 11578.

Schertler, G. F. X., Villa, C., & Henderson, R. (1993) *Nature 362*, 770.

Schwartz, T. W. (1994) *Curr. Opin. Biotechnol. 5*, 434.

Sealfon, S. C., Chi, L., Ebersole, B. J., Rodic, V., Zhang, D., Ballesteros, J. A., & Weinstein, H. (1995) *J. Biol. Chem. 270*, 16683.

Strader, C. D., Candelore, M. R., Hill, W. S., Sigal, I. S., & Dixon, R. A. F. (1989a) *J. Biol. Chem. 264*, 13572.

Strader, C. D., Sigal, I. S., & Dixon, R. A. F. (1989b) *FASEB J. 3*, 1825.

Strader, C. D., Gaffney, T., Sugg, E. E., Rios Candelore, M., Keys, R., Patchett, A. A., & Dixon, R. A. F. (1991) *J. Biol. Chem. 266*, 5.

Strader, C. D., Fong, T. M., Graziano, M. P., & Tota, M. R. (1995) *FASEB J. 9*, 745.

Straub, R. E., Frech, G. C., Joho, R. H., & Gershengorn, M. C. (1990) *Proc. Natl. Acad. Sci. U.S.A. 87*, 9514.

Suryanarayana, S., & Kobilka, B. K. (1993) *Mol. Pharmacol. 44*, 111.

Suryanarayana, S., Von Zastrow, M., & Kobilka, B. K. (1992) *J. Biol. Chem. 267*, 21991.

Vale, W., Grant, G., & Guillemin, R. (1973) in *Frontiers in Neuroendocrinology, 1973* (Ganong, W. F., & Martini, L., Eds.) pp 375−413, Oxford University Press, New York.

Wess, J., Maggio, R., Palmer, J. R., & Vogel, Z. (1992) *J. Biol. Chem. 267*, 19313.

Zhou, W., Flanagan, C., Ballesteros, J. A., Konvicka, K., Davidson, J. S., Weinstein, H., Millar, R. P., & Sealfon, S. C. (1994) *Mol. Pharmacol. 45*, 165.

BI952202R